

Deep exclusive electroproduction of π^+ from data measured with the HERMES detector at DESY

Murat M. Kaskulov* and Ulrich Mosel

Institut für Theoretische Physik, Universität Giessen, D-35392 Giessen, Germany

(Received 10 May 2009; published 31 August 2009)

Deeply virtual electroproduction of pions in an exclusive reaction $p(e, e'\pi^+)n$ is studied using a two-component model that includes soft hadronic and hard partonic reaction mechanisms. The results are compared with the experimental data measured at HERMES in the deep inelastic region for values of $Q^2 > 1 \text{ GeV}^2$ and $W^2 > 10 \text{ GeV}^2$. At forward angles the π^+ cross section is longitudinal and is dominated by exchange of Regge poles, with π being the dominant trajectory. The off-forward region with $-t > 1 \text{ GeV}^2$ is transverse and shows the dominance of partonic subprocesses. An implication of the present results for the future JLab facilities is briefly discussed.

DOI: [10.1103/PhysRevC.80.028202](https://doi.org/10.1103/PhysRevC.80.028202)

PACS number(s): 12.39.Fe, 13.40.Gp, 13.60.Le, 14.20.Dh

Exclusive electroproduction of pions in the reaction

$$e + N \rightarrow e' + \pi + N' \quad (1)$$

at high values of photon virtuality Q^2 and invariant mass W of produced hadronic final state provides an interesting tool to study a space-time pattern of partonic interactions in deep inelastic scattering (DIS). It may further reveal the partonic substructure of participating hadrons, correlating the longitudinal momentum fraction carried by quarks to transverse coordinates. This latter property of the hard exclusive reaction $N(e, e'\pi)N'$ follows from the QCD factorization theorem that was proven for hard $Q^2 \gg \Lambda_{\text{QCD}}^2$ electroproduction of mesons by longitudinal photons γ_L^* [1]. Predictions for the production by transverse virtual photons γ_T^* are absent because no factorization theorem has been proven for such photons. However, their contribution to the cross section is expected to be suppressed by at least a power of $1/Q^2$. Yet, above the resonance region $W^2 > 4 \text{ GeV}^2$ the exclusive reaction (γ^*, π^\pm) with charged pions provides important information concerning the electromagnetic form factor of the pion at momentum transfer Q^2 being much bigger than in the direct scattering of pions from atomic electrons [2].

Experimentally, the differential cross sections in the exclusive reaction $p(\gamma^*, \pi^+)n$ has been measured above the resonance region at CEA [3], Cornell [4], DESY [5], and recently at JLab [6]. At JLab a separation of cross sections into different transverse and longitudinal components has been carried out. The HERMES data at DESY [7] largely extend the kinematic region to much higher values of W toward the true DIS region $Q^2 \gg 1 \text{ GeV}^2$ and much higher values of $-t$. Theoretically, there is a long-standing issue concerning the reaction mechanisms contributing to the single pion $N(e, e'\pi)N'$ production at high energies and photon virtualities. Just above the resonance region around the onset of the deep inelastic regime the models describing the exclusive pion production $p(e, e'\pi^+)n$ in terms of hadronic degrees of freedom fail to reproduce the large transverse cross section σ_T observed in this reaction. For instance, the hadron-exchange

models, which are generally considered to be a guideline for the experimental analysis and extraction of the pion form factor, underestimate grossly σ_T at the highest values of Q^2 measured at JLab [6], whereas the longitudinal cross section σ_L was supposed to be well understood in terms of the pion quasi-elastic knockout mechanism [8]. This is because of the pion pole at low $-t$. Even at smaller DESY [5] and much higher Cornell [4] values of Q^2 there is a disagreement between model calculations based on the hadron-exchange scenario and experimental data. Another interesting example is the neutral pion production. In π^0 photoproduction the cross section is well described at high energies by exchange of Regge poles in the t channel, with ω and ρ being the dominant trajectories. This gives a natural explanation of the diffractive dip in the differential cross section at $-t \simeq 0.6 \text{ GeV}^2$ provided a *wrong signature zero* is accounted for in the Regge amplitudes. However, already at low values of Q^2 the experimental data indicate a sudden change in the reaction dynamics that washes out the diffractive dip. The nature of this transition is not fully understood within Regge phenomenology.

A possible solution of the σ_T problem at JLab was proposed in Ref. [9]. The approach followed there is to complement the hadron-like interaction types in the t channel, which dominate in photoproduction and low Q^2 electroproduction, by a direct interaction of virtual photons with partons followed by string (quark) fragmentation into π^+n . Then σ_T can be readily explained and both σ_L and σ_T can be described from low to high values of Q^2 . In Ref. [9] the reaction $p(e, e'\pi^+)n$ is treated as the exclusive limit, $z \rightarrow 1$, of the semi-inclusive reaction $p(e, e'\pi^+)X$ in DIS in the spirit of the exclusive-inclusive connection [10]. A suggestion concerning the partonic contribution to the exclusive reaction $N(e, e'\pi)N'$ follows the arguments in Ref. [11] where it has been shown that the typical exclusive photoproduction mechanisms involving a peripheral quark-antiquark pair in the proton wave function, the t -channel meson-exchange processes, should be unimportant in the transverse response σ_T already around $Q^2 \gtrsim 1 \text{ GeV}^2$ and play no role in the true deep inelastic region.

In this brief report we apply the two-component hadron-parton model proposed in Ref. [9] for the description of recent HERMES data to check its validity in a different kinematic

* murat.kaskulov@theo.physik.uni-giessen.de

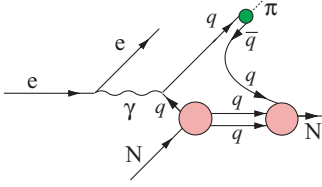


FIG. 1. (Color online) A schematic representation of the deeply virtual partonic part of the π -electroproduction mechanism. See the text for the details.

regime. We use the same model parameters as in Ref. [9]. In the model of Ref. [9] the hadron-exchange part is described by the exchange of Regge trajectories. In the reaction $p(\gamma^*, \pi^+)n$ we take into account the exchange of $\pi(140)$ - and $\rho(770)$ -meson Regge trajectories. The former one includes the electric part of the nucleon-pole contribution to conserve the charge of the system [12]. The partonic part is shown schematically in Fig. 1. It is a DIS like electroproduction mechanism where the quark knockout reaction $\gamma^*q \rightarrow q$ is followed by the fragmentation process of the Lund type [13]. We refer to Ref. [9] for further details. We recall that at JLab kinematics the transverse cross section is dominated by the mechanism described in Fig. 1. As a result the transverse cross section is large and at forward angles is comparable with the longitudinal cross section. As we shall see at HERMES, where the value of W is much larger, the transverse cross section gets much smaller at forward angles as compared to JLab data and the cross section is dominated by the exchange of Regge trajectories. However, the situation is different in the off-forward region. Because of the exponential fall-off of Regge contributions as a function of $-t$ the meson-exchange processes are negligible in the region of $-t > 1 \text{ GeV}^2$. In this region the interaction of virtual photons with partons gives the dominant contribution.

First, a brief discussion concerning some features of the HERMES data is in order. The differential cross section in the exclusive reaction $p(e, e'\pi^+)n$ can be written in the following form

$$\frac{d\sigma}{dQ^2 dv dt} = \frac{\pi\Phi}{E_e(E_e - \nu)} \left[\frac{d\sigma_T}{dt} + \varepsilon \frac{d\sigma_L}{dt} \right], \quad (2)$$

where the virtual photon flux is given by [14]

$$\Phi = \frac{\alpha}{2\pi^2} \frac{E_e - \nu}{E_e} \frac{\mathcal{K}}{Q^2} \frac{1}{1 - \varepsilon}, \quad (3)$$

with $\alpha \simeq 1/137$, $\mathcal{K} = \nu(1 - x_B)$, $\nu = E_e - E'_e$, and

$$\varepsilon = \frac{1}{1 + 2 \frac{\nu^2 + Q^2}{4E_e(E_e - \nu) - Q^2}} \quad (4)$$

is the ratio of longitudinal to transverse polarization of the virtual photon and other notations are obvious. At HERMES the kinematic requirement $Q^2 > 1 \text{ GeV}^2$ has been imposed on the scattered lepton to select the hard scattering regime. The resulting kinematic range is $1 < Q^2 < 11 \text{ GeV}^2$ and $0.02 < x_B < 0.55$ for the Bjorken variable. The measured cross sections are integrated over the azimuthal angle φ and a separation of the transverse and longitudinal parts was not feasible. Furthermore, the exclusive data were obtained from

π^+ semi-inclusive DIS data by using a model dependent subtraction procedure. The extraction of the HERMES data in Ref. [7] used the PYTHIA [15] event generator to subtract the non-exclusive background in the semi-inclusive π^+ measurement. By this it was supposed that the remaining signal in the HERMES data was not produced by the PYTHIA events and therefore it corresponds to the exclusive part, $z \simeq 1$, of the total π^+ semi-inclusive DIS cross section. Furthermore, HERMES found it necessary to change the default parameters in JETSET to describe the semi-inclusive DIS data in their kinematic regime [16]. With $E_e = 27.6 \text{ GeV}$ beam energy at DESY the ratio of longitudinal to transverse polarization of the virtual photon ε is high, $\varepsilon \simeq 0.95$. Contrary to JLab where ε is smaller the longitudinal cross section at HERMES enters the differential cross section with practically its full strength. The value of $s = W^2$ was required to be higher than 10 GeV^2 . To make a proper comparison with data the theoretical cross sections must be corrected for the bin size effect to account for the Q^2 and x_B dependence of the exclusive π^+ yield within the HERMES acceptance. The corresponding experimental distributions of π^+ as a function of Q^2 (left) and x_B (right) are shown in Fig. 2 and are used to generate the virtual photon flux in the Monte Carlo procedure to fold the theoretical cross sections.

Our results for the photon-nucleon differential cross section $d\sigma = d\sigma_T + \varepsilon d\sigma_L$ in the reaction $p(\gamma^*, \pi^+)n$ at HERMES are shown in Fig. 3. In Fig. 3 instead of t , the quantity $-t + t_{\min}$ is used, where $-t_{\min}$ denotes the minimum value of $-t$ for a given Q^2 and x_B . Different panels in Fig. 3 correspond to different Q^2 and x_B bins. The model results, which include both the hadron-exchange and partonic DIS contributions, are shown by the solid curves. We obtain satisfactory agreement with data for the first three (Q^2, x_B) bins and underestimate the cross section for the last bin with the highest values of Q^2 . Although with the model parameters at hand a perfect description of data can be achieved, we do not attempt to fit the data and use the same model parameters tuned to JLab data. The present description of exclusive π^+ DIS events does not employ the full PYTHIA machinery and uses in line with Ref. [9] the direct $\gamma^*q \rightarrow \pi^+q$ DIS mechanism to model the hard scattering regime: MSTP(14) = 26, PARP(91) = 1.2, MSTJ(17) = 1, MSTP(61) = 2, and MSTP(71) = 1 [15]. Of course, this calls into question the reliability of using the scattering of valence quarks only to describe the π^+ semi-inclusive DIS data at HERMES [16]. The idea followed here follows the exclusive-inclusive connection for a proper description of both exclusive and semi-inclusive DIS cross sections using the same fragmentation mechanism. However, modeling the transverse cross section by the hard DIS like processes, at forward angles we account for just a few percent of the exclusive π^+ cross section. As we shall see, the large part of the cross section at HERMES is dominated by exchanges of Regge poles that are missing in the generators like PYTHIA. At HERMES the exclusive cross section itself is only a few percent of the total π^+ semi-inclusive DIS cross section. Taking into account a subtraction procedure used at HERMES, at high values of $-t$ we describe the effects on the level of the subtraction and parameter dependent background.

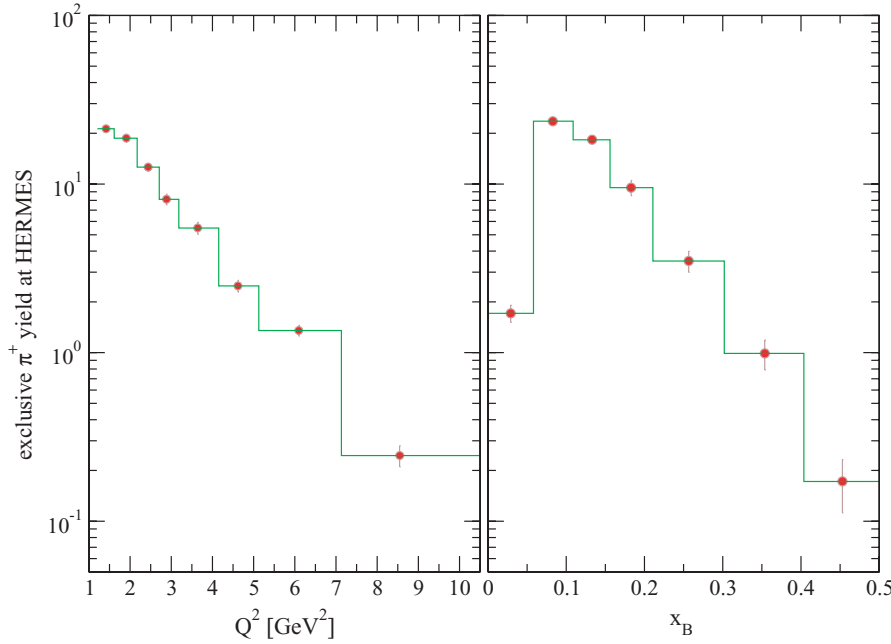


FIG. 2. (Color online) Distribution of exclusive π^+ events within the HERMES acceptance as a function of Q^2 and Bjorken scaling variable x_B .

Concerning different contributions to the cross section, in Fig. 3 the dash-dotted curves correspond to the exchange of the π -Regge trajectory and dash-dash-dotted curves to the exchange of the ρ -Regge trajectory. All the trajectories used here are linear. The histograms and dashed curves that just fit the histograms describe the hard partonic contributions in line with the DIS mechanism shown in Fig. 1 (for details, see Ref. [9]). As one can see, at forward angles the π exchange dominates the differential cross sections. The steep fall of $d\sigma/dt$ away from forward angles comes entirely from the rapidly decreasing π -exchange amplitude. The π exchange contributes mainly to the longitudinal response σ_L and at low momentum transfer $-t$ the variation of the cross section with Q^2 falls down as the electromagnetic form factor of the pion $\sigma_L \propto (F_{\gamma\pi\pi}(Q^2))^2$,

$$F_{\gamma\pi\pi}(Q^2) = (1 + Q^2/\Lambda_{\gamma\pi\pi}^2)^{-1}. \quad (5)$$

The value of the cutoff in Eq. (5) used in the calculations is $\Lambda_{\gamma\pi\pi}^2 = 0.52 \text{ GeV}^2$. This is an optimal value needed to describe the JLab data in the present model for values of $Q^2 \gtrsim 1.5 \text{ GeV}^2$. The magnitude of the cross section and the slope of solid curves and data at very forward angles are consistent with the Regge behavior,

$$d\sigma/dt \sim e^{2\alpha'_\pi \ln(s/s_0)(t-m_\pi^2) - 2\ln(s/s_0)}, \quad (6)$$

where $\alpha'_\pi = 0.7 \text{ GeV}^{-2}$ and $s_0 = 1 \text{ GeV}^2$. The contribution of the ρ exchange is marginal in σ_L and σ_T .

At large $-t$ the model cross section points mainly toward the direct coupling of the virtual photons to partons. Indeed, this is rather natural, because with increasing $-t$ at fixed Q^2 smaller distances can accordingly be accessed. This is opposed to t -channel meson-exchange processes that involve peripheral production of π^+ and therefore large distances

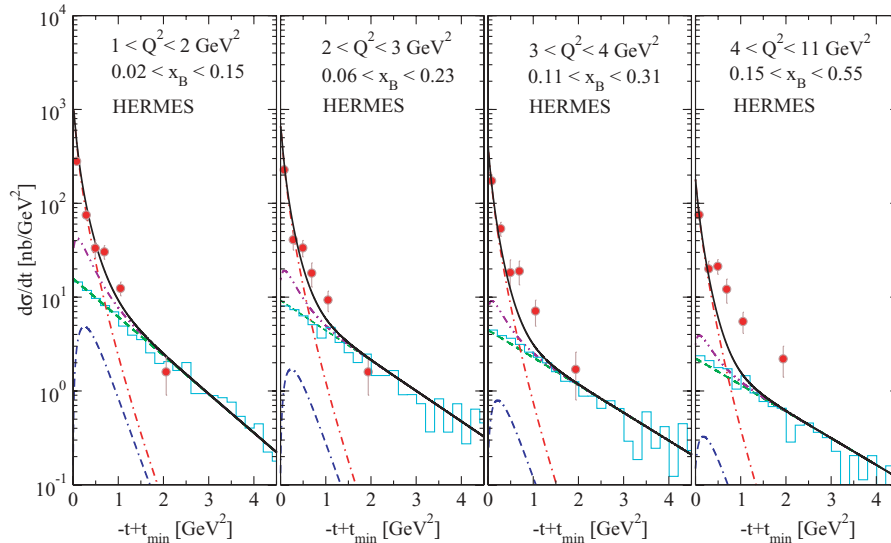


FIG. 3. (Color online) The differential cross section $d\sigma/dt = d\sigma_T/dt + \epsilon d\sigma_L/dt$ of the exclusive reaction $p(\gamma^*, \pi^+)n$ in the kinematics of the HERMES experiment. The solid curves are the model results. The dash-dotted curves correspond to the exchange of the π -Regge trajectory and dash-dash-dotted curves to the exchange of the ρ -Regge trajectory. The histograms and the dashed curves that just fit the histograms describe the partonic contributions in line with the DIS mechanism shown in Fig. 1. The dot-dot-dashed curves are the contribution of the transverse cross section $d\sigma_T/dt$ to the total unseparated response $d\sigma/dt$.

from the origin. At forward angles the DIS contribution (histograms in Fig. 1) to the cross section is smaller than the meson-exchange contributions by two orders of magnitude. However, the slope of the cross section in this case is also much smaller. Note that, in the model of Ref. [9] the partonic part is transverse and its behavior (slope) at forward angles is driven by the intrinsic transverse momentum distribution of partons $\sqrt{\langle k_T^2 \rangle} = 1.2$ GeV. From the fit to the histograms (dashed curves) we observe a slight decrease of the slope as a function of Q^2 but it is essentially the same as that at JLab energies. The partonic DIS part of the cross section shows a rather weak Q^2 dependence and has approximately the same order of magnitude for all Q^2 bins. The dot-dot-dashed curves in Fig. 1 are the contribution of the transverse cross section $d\sigma_T/dt$, which includes both Regge and hard partonic mechanisms, to the total unseparated differential cross section $d\sigma/dt$.

The partonic interpretation of the large $-t$ region proposed here is similar to the interpretation by Ref. [17] of HERMES data. In the latter work the pion form factor has been modified to account for different space-time patterns of hard interaction processes. However, there is an important difference. By modifying the off-mass-shell behavior of $F_{\gamma\pi\pi}(Q^2)$ at large $-t$, see Eq. (5) with $\Lambda_{\gamma\pi\pi} \rightarrow \Lambda_{\gamma\pi\pi}(t, Q^2)$, one essentially modifies the dominant longitudinal component and absorbs the partonic contributions in σ_L . Our interpretation relies on the DIS like $\gamma^*q \rightarrow q$ interaction that shows up in the transverse response σ_T as in any high (Q^2, W) DIS processes.

The considerable reduction of the transverse exclusive cross section as a function of W observed here has important consequences for the future JLab facilities. For instance, in Fig. 4 we show the longitudinal hadronic and transverse partonic cross sections at values of $Q^2 = 1.5$ GeV² and for two different values of W , $W = 2$ and 3 GeV. The transverse cross section (top histogram) at present JLab energies ($W = 2$ GeV) is largely in agreement with data and at forward directions is comparable in order of magnitude with the longitudinal cross section (dashed curve). An increase of W from just 2 to 3 GeV reduces the transverse DIS cross section by about two orders of magnitude. However, the longitudinal cross section is barely changed. This may support QCD based calculations that rely on small transverse components in an extraction of the nucleon's generalised parton distributions (GPD). This example also shows that at JLab with a 12 GeV electron beam an extraction of the pion charge form factor from forward exclusive electroproduction data will not be

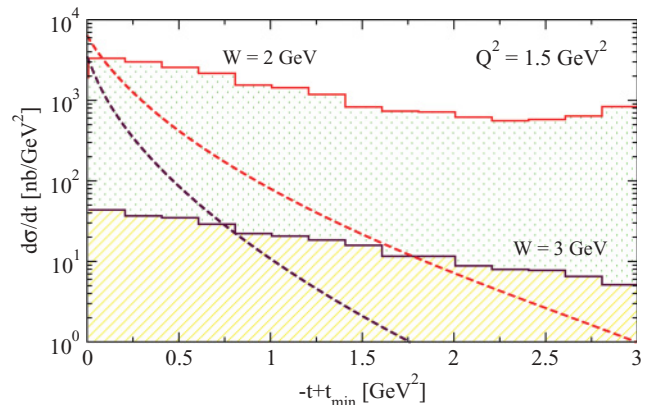


FIG. 4. (Color online) The transverse DIS (histograms) and longitudinal Regge-exchange (dashed curves) differential cross sections in the exclusive reaction $p(\gamma^*, \pi^+)n$ for the fixed value of $Q^2 = 1.5$ GeV² and for different values of W , $W = 2$ GeV (top) and $W = 3$ GeV (bottom).

contaminated by the large transverse non-pole background contributions. Furthermore, at these energies the theoretical analysis and proof of the color transparency signal observed in semi-exclusive ($e, e'\pi^+$) off nuclei will be considerably simplified [18,19].

In summary, we applied the model of Ref. [9] to recent HERMES data on exclusive π^+ electroproduction in the deep inelastic region. The data were obtained at much higher values of Q^2 and W as compared to the previous data from JLab. We find that the transverse cross section, which is large at JLab, gets much smaller at HERMES. However, with increasing $-t$ the role of partonic DIS mechanisms becomes more pronounced. We also find that the forward production of π^+ at HERMES is dominated by the exchange of Regge poles, with π being the dominance trajectory. On the contrary, the off-forward region with $-t > 1$ GeV² is dominated by partonic interactions describing the direct coupling of virtual photons to constituents of the nucleon. For future JLab energies the model predicts a tiny transverse component that might be important for the GPD interpretation of $p(\gamma^*, \pi^+)n$ as well as in the extraction of the pion form factor from the forward electroproduction data.

We are grateful to Dr. A. Airapetian for helpful communications and for making the actual ($Q^2, x_B, -t$) values of the data available to us. This work was supported by BMBF.

[1] J. C. Collins, L. Frankfurt, and M. Strikman, Phys. Rev. D **56**, 2982 (1997).
[2] J. D. Sullivan, Phys. Lett. **B33**, 179 (1970).
[3] C. N. Brown *et al.*, Phys. Rev. D **8**, 92 (1973).
[4] C. J. Bebek *et al.*, Phys. Rev. D **17**, 1693 (1978).
[5] P. Brauel *et al.*, Phys. Lett. **B69**, 253 (1977).
[6] H. P. Blok *et al.*, Phys. Rev. C **78**, 045202 (2008).
[7] A. Airapetian *et al.*, Phys. Lett. **B659**, 486 (2008).
[8] V. G. Neudatchin *et al.*, Nucl. Phys. **A739**, 124 (2004).
[9] M. M. Kaskulov, K. Gallmeister, and U. Mosel, Phys. Rev. D **78**, 114022 (2008).
[10] J. D. Bjorken and J. B. Kogut, Phys. Rev. D **8**, 1341 (1973).

[11] O. Nachtmann, Nucl. Phys. **B115**, 61 (1976).
[12] M. Vanderhaeghen, M. Guidal, and J. M. Laget, Phys. Rev. C **57**, 1454 (1998).
[13] B. Andersson *et al.*, Phys. Rep. **97**, 31 (1983).
[14] L. N. Hand, Phys. Rev. **129**, 1834 (1963).
[15] T. Sjostrand *et al.*, J. High Energy Phys. 05 (2006) 026.
[16] A. Hillenbrand, Ph.D. thesis, 2005; www-hermes.desy.de/notes/pub/doc-public-status.html.
[17] J. M. Laget, Phys. Rev. D **70**, 054023 (2004).
[18] B. Clasie *et al.*, Phys. Rev. Lett. **99**, 242502 (2007).
[19] M. M. Kaskulov, K. Gallmeister, and U. Mosel, Phys. Rev. C **79**, 015207 (2009).